Available online at www.sciencedirect.com
ScienceDirect
Biochimica et Biophysica Acta 1768 (2007) 13–20
Biochimica et Biophysica Acta BBA
www.elsevier.com/locate/bbamem

Quantifying the effects of melittin on liposomes

J.F. Popplewell [a], M.J. Swann [a,*], N.J. Freeman [a], C. McDonnell [b], R.C. Ford [b]

[a] *Farfield Scientific Ltd, Farfield House, Southmere Court, Electra Way, Crewe Business Park, Crewe CW1 6GU2, UK*
[b] *Faculty of Life Sciences, University of Manchester, Manchester, M60 1QD*

Received 16 September 2005; received in revised form 12 May 2006; accepted 19 May 2006
Available online 23 May 2006

Abstract

Melittin, the soluble peptide of bee venom, has been demonstrated to induce lysis of phospholipid liposomes. We have investigated the dependence of the lytic activity of melittin on lipid composition. The lysis of liposomes, measured by following their mass and dimensions when immobilised on a solid substrate, was close to zero when the negatively charged lipids phosphatidyl glycerol or phosphatidyl serine were used as the phospholipid component of the liposome. Whilst there was significant binding of melittin to the liposomes, there was little net change in their diameter with melittin binding reversed upon salt injection. For the zwitterionic phosphatidyl choline the lytic ability of melittin is dependent on the degree of acyl chain unsaturation, with melittin able to induce lysis of liposomes in the liquid crystalline state, whilst those in the gel state showed strong resistance to lysis. By directly measuring the dimensions and mass changes of liposomes on exposure to melittin using Dual Polarisation Interferometry, rather than following the florescence of entrapped dyes we attained further information about the initial stages of melittin binding to liposomes.

Keywords: Liposome; Phospholipid; Bilayer; Melittin; Lysis

1. Introduction

Melittin is a 26 amino acid, amphipathic peptide, with 6 positive charges [1]. The amino-terminal is composed predominantly of hydrophobic amino acids [2] (residues 1–20), whereas the carboxy-terminal end has a stretch of predominantly hydrophilic amino acids (residues 21–26), which give rise to its amphiphilic character [3]. It is known for its strong interaction with membranes, making it a popular agent for studying peptide–lipid interactions. Its charged nature makes it water soluble and yet it associates with natural and artificial membranes binding to them as an amphipathic alpha helix [4,5], having been shown to bind to both electrically neutral and negatively charged lipid bilayers [1,6]. Although melittin is lytic to a variety of cell types, the degree of vesicle leakage produced by melittin depends on the bilayer lipid composition. Melittin reaches membranes through the aqueous phase so a consideration of its properties in aqueous solutions is relevant to its effects on membranes. In common with other membrane binding peptides and membrane proteins, it is predominately hydrophobic, and in aqueous solution it is either monomeric or associated as a tetrameric aggregate. The aqueous monomer has no detectable secondary structure, as determined by circular dichroism [7,8], and high resolution ^{1}H NMR [9] shows shifts typical of random coil polypeptides. The monomer has been described as rod-like with dimensions 3.5 nm × 1.2 nm. By contrast the tetramer shows melittin to be in a predominantly helical conformation, with factors that suppress charge, such has high ionic strength, leading to self association.

The organisation of membrane-bound melittin is dependent on the physical state and composition of the membranes, thus in addition to studying the interaction of melittin with liposomes composed of differing phospholipid headgroups, we also used melittin to address the influence of unsaturated lipids in modulating lipid peptide interactions. In a wider context the importance of understanding melittin membrane interactions arises from the observation that the amphiphilic alpha-helical conformation of this haemolytic toxin in membranes resembles those of signal peptides [10] and that melittin mimics the N-terminal of HIV-1 virulence factor Nef1–25 [11].

* Corresponding author.
E-mail address: mswann@farfield-sensors.com (M.J. Swann).

0005-2736/$ - see front matter © 2006 Elsevier B.V. All rights reserved.
doi:10.1016/j.bbamem.2006.05.016

1.1. Effect of melittin on phosphatidyl choline (PC) liposomes

An investigation of vesicles composed of different phosphatidylcholines [12] revealed that the extent of leakage of internal contents induced by melittin can range from practically none to essentially complete, depending upon the fatty acyl chain composition of the phospholipid. The extent of leakage was shown to increase with the number of double bonds in the series dioleoylphosphatidylcholine (number of carbon atoms in the chain: no of double bounds in the chain = 18:1) <dilinoleoylphosphatidylcholine (18:2) <dilinolenoylphosphatidylcholine (c18:3). It was also shown to depend on the length of the saturated chain with 1-myristoyl-2-arachidonoylphosphatidylcholine (14:0, 20:4) vesicles being more sensitive to melittin induced leakage than 1-palmitoyl-2-arachidonoylphosphatidylcholine (16:0, 20:4), 1-stearoyl-2-arachidonoylphosphatidylcholine (18:0, 20:4) or 1-palmitoyl-2-docosahexaenoylphosphatidylcholine vesicles (16:0, 22:6). Among the lipids examined, diphytanoylphosphatidylcholine (4 ME, 16:0) vesicles were shown to be the least susceptible to melittin induced leakage. The results indicated that lipid fatty acyl structure may be important in lipid–protein interactions of the kind simulated by melittin [13].

It was shown that melittin association with phosphatidylcholine membranes takes place in the order of milliseconds. The kinetics of this phenomenon is still a matter of controversy as it is reported to be monophasic by some researchers [14,15], and biphasic by others [16,17].

1.2. Effect of negatively charged lipids

A number of publications have described how the presence of negatively charged lipids in the liposomes inhibits the lytic capabilities of melittin. Whilst the presence of negatively charged lipids in the membranes increases the membrane affinity of melittin [18–20], it anchors the peptide at the interface, preventing the reorganisation required to induce lysis [21–23]. In addition to verifying the protective effect of negative lipids via a technique other than fluorescence detection of entrapped dyes we have studied the fate of melittin associating with negatively charged lipids.

1.3. Quantifying changes in the liposomes

Much of the work published on melittin has made use of entrapped fluorescent dyes, with the lysis of liposomes followed by measuring the release of the entrapped dye. In the work described here we employ a surface-based technique called dual polarisation interferometery (DPI) which permits the user to measure the changes in thickness, refractive index and mass of materials 100 nm thick or less on the surface of a glass waveguide [24]. The dual slab waveguide is illuminated with laser light of alternating polarisations at one end, and as the light exits the 2 waveguides at the other end they interfere to produce an interference pattern (see Fig. 1). The waveguide structure is integrated with a fluidic system permitting the continuous flow of material over the top waveguide, and as material is added to or removed from the waveguide, the interference pattern moves, and these changes in the position of the interference pattern can be "resolved" into changes in thickness, RI and mass of the material on the waveguide [25–28]. Thus if a population of 50 nm liposomes is immobilised onto the waveguide surface, the dimensions of the layer will be measured at 50 nm (assuming no deformation of the liposomes on binding to the waveguide), there will be a surface coverage value (in ng/mm^2) and a refractive index of the layer, which will reflect the density of liposome packing. We have also used dynamic light scattering (DLS) and transmission electron microscopy (TEM) to study the liposomes. The combination of these three techniques, performed on the same systems, provides a detailed picture of the events of melittin association.

2. Materials and methods

2.1. Materials

All phospholipids were purchased from Avanti Polar Lipids (Birmingham, AL, USA). Melittin, Phosphate buffered saline (PBS), NaCl were purchased

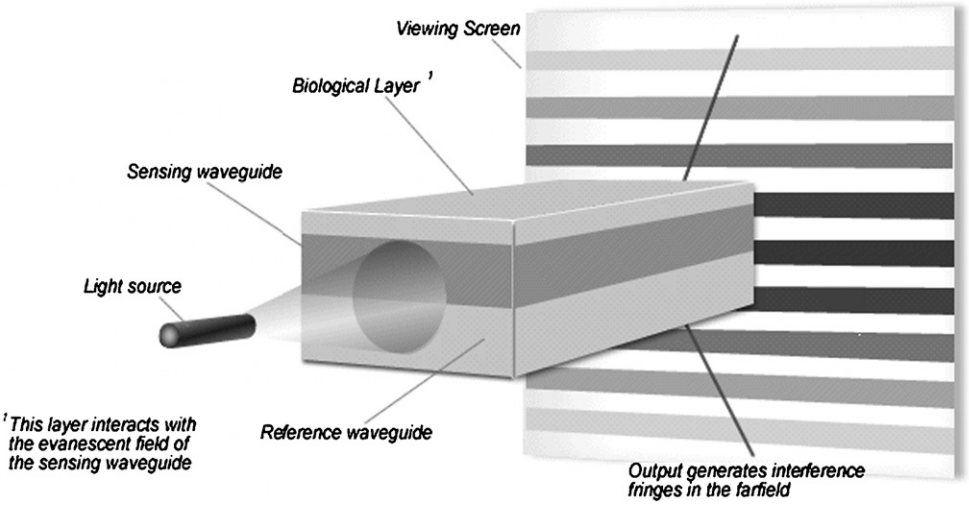

Fig. 1. DPI utilises polarised light from a laser passing down a waveguide onto which a biological layer has been deposited. The evanescent field emanating out of the waveguide interrogates the biological layer.

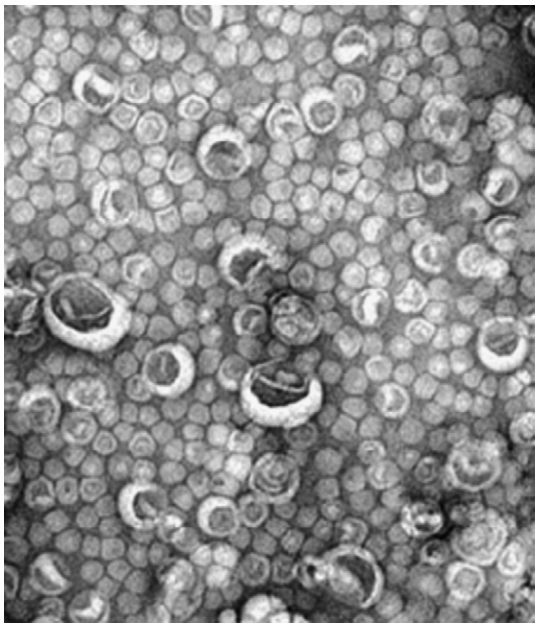

Fig. 2. DMPC Liposomes at 2 mg/ml, stained by 12% (w/v) ammonium molybdate with TEM micrographs taken on a Philips Tecnai 10, magnification 53,000x.

from Sigma (Dorset, UK), water (HPLC grade) and ethanol (HPLC grade) were purchased from Fisher Scientific UK Ltd. (Loughborough, UK).

2.2. Methods

2.2.1. Preparation of liposomes via hydration and sonication

Liposome preparation via hydration and sonication was carried out according to procedures modified from literature [29–34] for the preparation of small (<100 nm liposomes) and the same basic preparation method applied to all liposomes regardless of lipid composition. Lyophilized lipid powders were hydrated via mixing with PBS (2 mg/ml), during which the dried lipid film swells with bilayer stacks. The hydrated sheets detach during on-going agitation and self close to form vesicles which prevent the interaction of water with the hydrocarbon core of the bilayer at the edges. Typically a hydration time of 1 h with vigorous stirring was employed, resulting in a uniform suspension. Sonic energy was employed to disperse the larger liposomes into smaller ones, with the lipid suspension placed in a test tube in the bath sonicator (Branson 200, Soest, Holland), and sonicated until the solution changes from milky to nearly clear solution.

2.2.2. Liposome preparation via surfactant removal

Liposome samples prepared by dissolving approximately 3 mg of lipid in 100 μl 1:1 Chloroform:ethanol mix which was then dried to a thin film in a stream of N_2. To the dried film 10% (v/v) n-dodecyl-beta-maltoside (DDM, 27 μl) was added, followed by buffer to make the lipid concentration 0.5 mg/ml. To the lipid/surfactant solution 30 s cycles of vortexing and sonication were employed until the solution was clear. Next surfactant adsorbing Bio-Beads SM-2 (Bio-Rad, Hercules, California, USA) were added at a concentration of 225 mg/ml and left rotating at 4 °C for 16 h, after which the beads were skimmed from the surface of the sample.

2.3. Liposome sizing on a solid support via Dual Polarisation Interferometry (DPI)

All DPI measurements were performed on an AnaLight Bio200 (Farfield Scientific, Crew, UK) equipped with a 632.8 nm laser. Depending on the liposome composition the instrument was fitted with either a silicon oxynitride waveguide surface or an amine functionalised waveguide surface, and perfused with PBS. The instrument is a dual channel system, with each 2 μl cell perfused at 12.5 μl/min and maintained at 20 °C. Following calibration steps to check the refractive index of the PBS running buffer, liposome solutions were perfused over the waveguide surface at 25 μl/min until a steady state response was attained (typically 5–10 min, depending on the phospholipid).

Stable liposome layers were challenged with melittin (0.5 mg/ml) at the same flow rate for 2 min (total volume 50 μl), then following a period of washing, 1 M NaCl (2 min, 50 μl).

2.4. Size distribution of liposomes in solution (DLS)

Mean liposome size was determined by dynamic light scattering with a Malvern Zetasizer 3000 using a 5 mW He–Ne laser and the Windows PCS version 1.31 software (Malvern Laboratories Ltd., Malvern, UK).

2.5. Transmission electron microscopy of liposomes

In preparation for liposome addition, TEM 400 mesh copper grids (S160-4, Agar Scientific) were negatively charged by glow discharge (Cressington 208, Watford, UK). Liposomes at 2 mg/ml (3 μl) were incubated with the grids (60 s), after which the grids were gently blotted dry, and after 2 wash steps with distilled water, the sample was stained by addition of 12% (w/v) ammonium molybdate for varying times (20–30 s) before again being gently blotted dry. Micrographs were taken on a Philips Tecnai 10 on Kodak SO-163 film, and micrographs were scanned with a UMAX Photolook scanner with 256 grey levels.

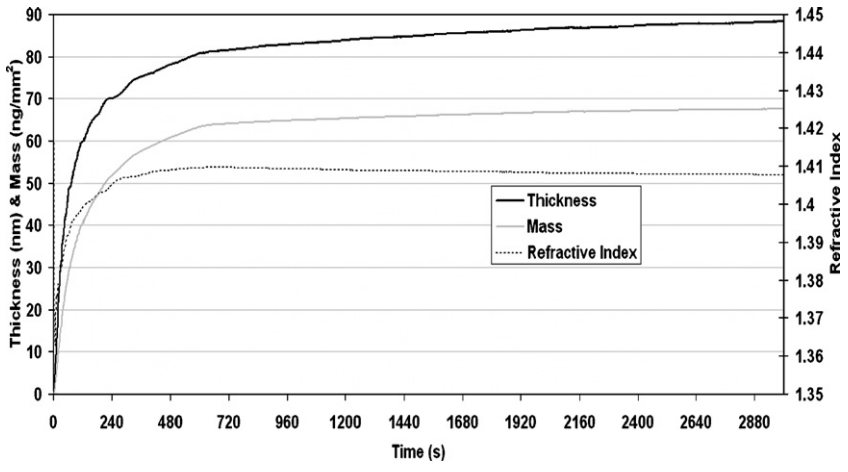

Fig. 3. Shows the parameters generated when DPI is applied to the measurement of liposomes added to a solid substrate, namely the thickness, refractive index and mass of a layer of DSPA liposomes added to an unmodified, silicon oxynitride surface at a flow rate of 25 μl/m.

3. Results

3.1. Liposome visualisation via TEM and DLS

Prior to immobilisation on the solid substrate, selected liposome solutions prepared according to Sections 2.2.1 and 2.2.2 were sized via DLS and micrographs were recorded in the TEM. Using low volume disposable sizing cuvettes the liposome solutions without any further treatment were sized via DLS at 20 °C with the sizing presented using Malvern Instruments "number" function, which takes account of the disproportionate scatter from a very small percentage of larger particles. 1,2-Dioleoyl-*sn*-Glycero-3-Phosphocholine (DOPC) liposomes prepared with protocol 2.2.1 were sized at 40.2±12.9 nm, 1,2-Dipalmitoyl-*sn*-Glycero-3-Phosphocholine (DPPC) vesicles were 47.6±10.4 nm and 1,2-Distearoyl-*sn*-Glycero-3-Phosphate (DSPA) vesicles were 83.8±16.7 nm.

Examination of the liposome population via TEM revealed the liposomes exist as predominately monodispersed liposomes. 1,2-Dipalmitoyl-*sn*-Glycero-3-[Phospho-L-Serine] (DPPS) liposomes were measured with an average diameter 46±29 nm, with a few, very large (> 100 nm) liposomes per micrograph (micrograph field size ca. 1000×1000 nm). DSPA vesicles were also predominately monodisperse, with an average diameter of 53±22 nm, with 1–2 "stacks" (deformed liposomes stacked on top of each other without fusing) per micrograph. Thus broadly as measured via DLS, we can characterise two principal populations present, small (20–80 nm) monodisperse liposomes, making up ≥95% of the liposome population, with the remaining 5% a combination of large, monodisperse liposomes and stacked liposomes. Fig. 2 shows a representative micrograph of 1,2-Dimyristoyl-*sn*-Glycero-3-Phosphocholine (DMPC) liposomes.

3.2. Dimensions of liposomes immobilised on a solid substrate

Fig. 3 shows a typical deposition profile measuring changes in thickness, refractive index (RI) and mass as a DSPA liposome layer is assembled on the surface of the functionalised DPI waveguide surface substrate, with mass values generated taking the RI of the lipid to be 1.435 and the density to be 1.05 g/cm^3 [3] giving a Refractive Index Increment (RII) of 0.0955 cm^3/g. The final layer thickness is 88 nm, which when compared to the DLS value of 83 suggests there is little deformation when DSPA liposomes (Tm 75 °C) assemble onto the solid substrate. This deposition profile contrasts with the layer thickness obtained when low transition temperature lipids are deposited on a solid substrate. As can be seen from Fig. 4, the DOPC (Tm − 20 °C) liposome layer thickness is considerably thinner than the diameter measured via DLS and TEM. A summary of a range of experiments with typical liposome values formed from DOPC, DMPC, 1-Palmitoyl-2-Oleoyl-*sn*-Glycero-3-Phosphocholine (POPC), DPPC, DPPS, DSPA, 1,2-Distearoyl-*sn*-Glycero-3-[Phospho-rac-(1-glycerol)] (DSPG), and mixed lipid systems from Phosphatidylethanolamine (PE)/PG/cholesterol is given in Table 1. The thickness value is the average thickness of the layer deposited, and the RI values give an indication as to the lipid: buffer ratio in the liposomes. The RI of PBS is 1.3348, whilst that for phospholipid is 1.435–1.45 [35,36] thus liposome layers with refractive indices close to buffer (1.35–1.37) can be considered as being formed predominately by unilamellar vesicles, whilst those with RI 1.38 and higher are likely to contain

Table 1
The dimensions of liposomes, as measured via DPI, immobilised on a solid substrate

Phospholipid	Thickness (nm)	Refractive index	Mass (ng/mm^2)
DOPC	18.5	1.375	7.8
DSPA	87.0	1.408	67.1
DPPS	36.6	1.392	22.1
DSPG	45.7	1.398	30.5
DPPC	33.9	1.367	11.5
DMPC	43.3	1.348	5.8
POPC	25.6	1.376	11.1
PE/PG/Cholesterol	22.0	1.359	5.6

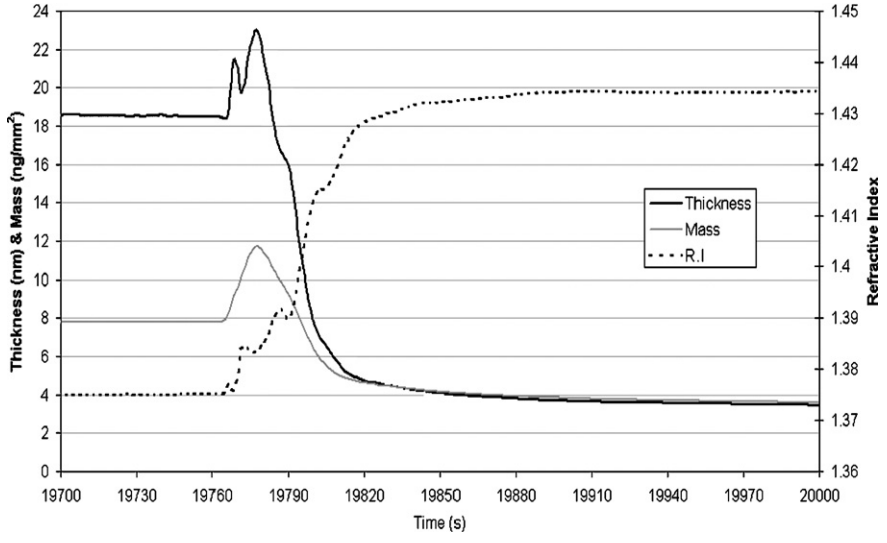

Fig. 4. The effect of an injection of melittin (0.5 mg/ml) on the dimensions of an immobilised layer of DOPC liposomes. On addition of melittin there is an initial increase in refractive index, mass and thickness as the melittin associates with DOPC, followed by a rapid decrease in both mass and thickness as the liposome ruptures.

more lipid and less buffer per liposome and thus to some degree are multilamellar. A full description of different liposome preparation techniques to engineer different number of lamellae and converting RI into a prediction for the number of lamellae is beyond the scope of the present paper, and will be described separately (Freeman et al, submitted).

3.3. Effects of melittin on PC liposomes

Addition of DOPC liposomes to the solid substrate shows the generation of a very stable layer, but radical changes to this layer occur upon addition of melittin as shown in Fig. 4. The data obtained here on addition of a relatively high melittin concentration (0.5 mg/ml) shows the kinetic progression of the different stages of melittin/liposome interaction. This concentration is used to in effect saturate each process, and so provide useful stoichiometric data at the transition points between the different phases of a multiphasic process. On addition of melittin there is an initial increase in refractive index, mass and thickness. There is a maximum in the mass and thickness followed by a rapid decrease in both, occurring over a period of a few seconds, together with a continued increase in the refractive index. The maximum in the mass corresponds to an addition of approximately one melittin molecule per twelve lipid molecules (using a RII value for the melittin of 0.186 cm^3/g, a value typically used for protein; the plotted mass is based on the lipid RII values). Thus it would appear that melittin binds to the liposome, giving a thickness and mass increase, and then once sufficient numbers of melittin molecules have associated with the DOPC liposome, it ruptures leading to a rapid decrease in measured thickness and a decrease in mass. The refractive index is observed to rapidly increase concurrently with the thickness decrease. This would be consistent with an aqueous filled liposome losing its aqueous content on lysis and the melittin containing wall collapsing onto the surface. The measured dimensions of the remaining layer on the surface are consistent with a single bilayer with a thickness of 4 nm [37] and a refractive index of 1.435 [35,36]. The absence of any remaining intact liposomes was verified by the absence of a further thickness decrease upon a second addition of melittin, with the liposome population lysed upon a single injection.

When the experiments were performed with DPPC liposomes the lytic activity of melittin was almost completely inhibited with the liposome layer retaining close to its original thickness after two consecutive melittin injections (Fig. 5). As for DOPC liposomes, the addition of melittin results in a mass increase during the first few seconds, but in contrast the increase is small, as is the increase in RI and decrease in thickness. There is no substantial decrease in mass or thickness at any stage after the melittin addition. The layer thickness is observed to decrease slightly from 27 nm to 25.5 nm, but clearly the liposomes have maintained their structure. There is a significant increase in refractive index and mass, implying that the melittin does associate with the phospholipid, but lysis is not induced. The additional mass bound to the DPPC liposomes corresponds to approximately one melittin per 60 DPPC molecules.

3.4. Effect of melittin on negatively charged liposomes, PS, PG and PA

As with PC, liposomes formed with other lipids such as PS, PG and PA formed stable layers with dimensions on the solid substrate comparable with sizes determined via DLS and as visualised via TEM. As can be seen from Fig. 6 there is considerable binding of melittin to the 37 nm negatively charged liposomes as evidenced by a substantial increase in measured surface mass. Examining the changes in RI and thickness reveals a substantial increase in thickness, to over 50 nm. This increase in thickness is observed to be stable. The RI can be seen to increase rapidly to a maximum corresponding to the point at which the thickness is at a minimum and then to stabilise and reduce slightly as the thickness increases. The mass gain that has taken place at the minimum in the thickness corresponds to one melittin per approximately 30 lipid molecules, and at the end of the binding process, one melittin per six lipid molecules. To test whether the thickness increase could have been induced by

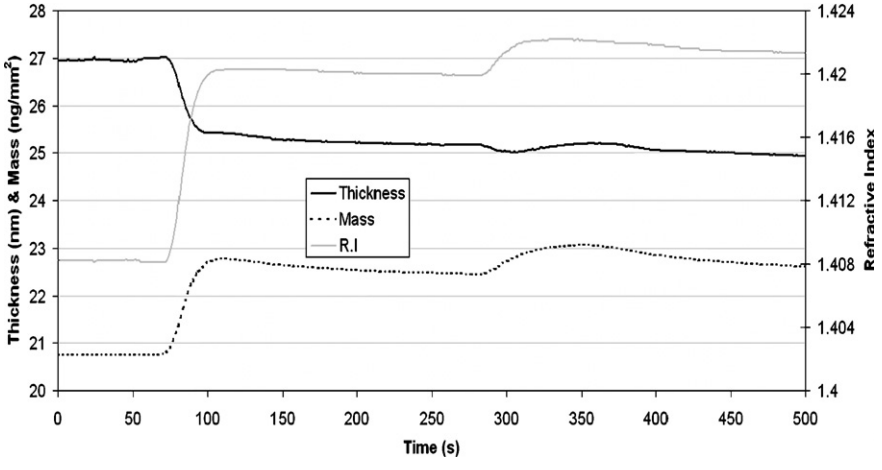

Fig. 5. The effect of sequential injections of melittin (0.5 mg/ml) at 50 s and 270 s on the dimensions of a layer of DPPC liposomes immobilised on a silicon oxynitride waveguide. The addition of melittin results in a mass increase during the first few seconds, but there is no substantial decrease in mass or thickness at any stage after the melittin addition, with the liposomes evidently maintaining their structure.

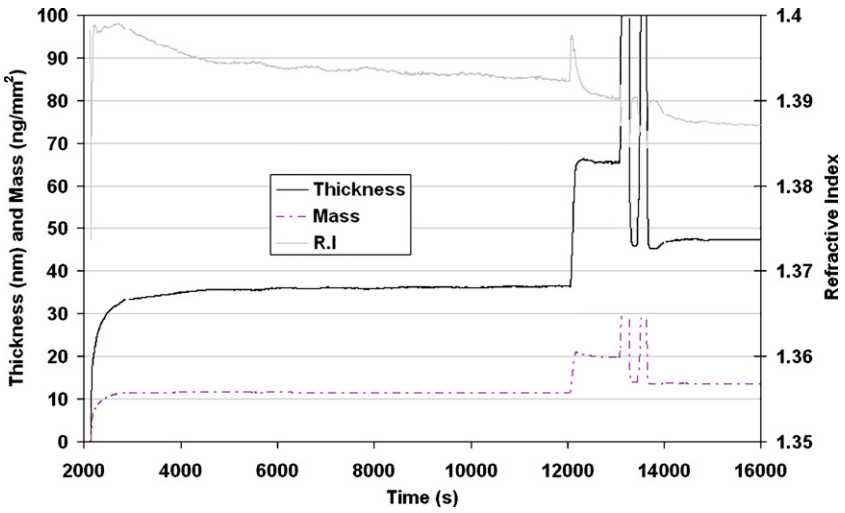

Fig. 6. The effect of an injection of melittin at 12000 s (0.5 mg/ml) then 2 sequential injections of 1 M NaCl on the dimensions of an immobilised layer of DSPG liposomes. As can be seen from the figure, there is considerable binding of melittin to the 37 nm negatively charged liposomes as evidenced by a substantial increase in measured surface mass and thickness. Upon addition of salt the mass, thickness and RI returned back close to the original value, indicating that the bound melittin had been displaced and the liposome structure was also essentially the same as that pre-melittin.

melittin fusing adjacent liposomes and/or whether it was purely a result of melittin binding via an electrostatic driven interaction (see above) 1 M NaCl was injected to shield lipid/peptide charge–charge attraction. The mass, thickness and RI returned back close to the original value, indicating that the bound melittin had been displaced and the liposome structure was also essentially the same as that pre-melittin, thus probably excluding fusion as the mechanism for the thickness increase and also indicating that the melittin DSPG interaction is predominantly electrostatic in nature. These changes of a small initial thickness decrease followed by a significant thickness increase were also observed for liposomes formed with DPPS and DSPA (data not shown), with the changes reversed by an injection of salt in each case (see Fig. 6).

4. Discussion

Although cell lysis by melittin has been extensively studied, the molecular mechanism of its hemolytic activity is not well understood. In particular, the role of specific lipids on melittin-induced hemolysis is not yet clear. The action of melittin in membranes is believed to be independent of any receptors [1,38,39], and in this paper we focused on the modulatory role of different lipids on membrane melittin interactions. The data presented show that both melittin binding and melittin-induced lysis is strongly dependant on the bilayer lipid composition, with the data demonstrating that specific lipid components of plasma membranes can provide protection against melittin-induced leakage.

Melittin has previously been shown to form pores in lipid bilayers that have been described in terms of at least two different structural models. In the “barrel stave” model the bilayer remains more or less flat [33], with the peptides penetrating across the bilayer hydrocarbon region and aggregating to form a pore, whereas in the “carpet” model melittin binds electrostatically to the outside of the membrane, aligning parallel to the membrane, covering it in a carpet like manner. Upon reaching a threshold concentration membrane penetration occurs resulting in membrane disruption and micellization. An intermediate step in the “carpet” model is the formation of pores, known as “toroidal” pores which induce defects in the bilayer such that the bilayer bends sharply inward to form a pore lined by both peptides and lipid headgroups [40]. Proponents of both models agree the mechanism must be “all or none” and predicts the co-existence of 2 different vesicle populations, the lysed and intact.

4.1. Actions of melittin on PC liposomes

Experiments with cholesterol indicate that the area per lipid hydrocarbon chain and the related area compressibility modulus are key factors that affect melittin–lipid interactions, with the introduction of cholesterol shown to reduce the area per lipid hydrocarbon chain [41,42] and increase the area compressibility modulus [43]. Both the area per lipid hydrocarbon chain and the compressibility modulus would be expected to influence the partitioning of amphipathic peptides into the interfacial region of the bilayer. As the area per lipid hydrocarbon chain decreases, less of the bilayer hydrocarbon surface is exposed to the peptide, which decreases the hydrophobic attraction of the peptide to the bilayer. The area compressibility modulus is related to the energy needed to change the area per lipid molecule. Since the bilayer surface must expand in order to incorporate the amphipathic peptide melittin, the larger the value of compressibility modulus the more energy is required to partition melittin into the bilayer. The results presented here strongly suggest that under the conditions used the liquid crystalline state of DOPC, with its low compressibility modulus, permits the insertion of melittin, disrupting the alignment of the hydrocarbon chains and inducing membrane lysis. For DPPC, in the gel state at room temperature, its higher compressibility modulus [44] prevents the insertion of melittin to a sufficient degree for the liposome to undergo fatal lysis. Additions of melittin made over a range of concentrations,

0.1–2.5 mg/ml to DPPC established melittin does not induce lysis over a range of lipid:melittin ratios.

The details of the melittin interaction with DOPC and DPPC warrant some detailed comparison. DPPC proceeds via a simple single stage process causing a small decrease in the total liposome thickness and modest mass uptake limiting at one melittin (26 amino-acids) per 60 lipid molecules or ~ 30 lipid molecules forming the outside of the bilayer. If the process were solely driven by charge interaction of the 6 positive amino acid residues with the lipid phosphatidyl groups, this stoichiometry might be expected to be higher, as in the case of DOPC or indeed DSPG. In the case of DPPC however it can be postulated that the higher (than DOPC) compressibility modulus prevents melittin tail insertion, whilst the positive choline outer headgroup confines the melittin to be bound within the lipid head region and so limiting the available volume available for melittin uptake. The observed compression of the liposome layer is consistent with this, possibly reflecting a melittin induced bridging of adjacent lipid phosphatidyl groups causing a tightening of the bilayer membrane structure. In the case of DOPC insertion of the hydrophobic melittin tail into the lipid bilayer is much easier, and proceeds to allow more space within the lipid head region for each phosphatidyl group to coordinate one of the 6 positive amino-acids in a melittin molecule. Insertion of the melittin tail into the lipid bilayer core would be expected to produce an increase in liposome wall volume which translates into an increase of liposome thickness, which is indeed measured. DOPC vesicle disruption is seen to take place at the point at which the melittin stoichiometry exceeds one per 12 lipids (~ one melittin per 6 lipid molecules in the outer membrane layer). This is significant, because it reflects the point at which the outer membrane has no more available uncoordinated phosphatidyl groups, and additional melittin insertion would no longer be driven by an anchored, oriented process, but must involve restructuring of the bilayer, as is observed in the breakdown of the liposomal structure.

Thus the progressive interaction of melittin with DOPC can be postulated to proceed in a three stage process, namely: (i) rapid adsorption into the base of the lipid headgroup region (cf DPPC), (ii) continued and significantly greater adsorption accompanied by melittin reordering via tail insertion into the lipid bilayer core and (iii) breakup of bilayer structure once the melittin: PC ratio exceeds 1:6. It must be noted that the point at which the permeability of liposomes (whether by pore formation or not) increases occurs in this scheme cannot be categorically defined, as 'pores' are likely be formed within the liposome structure at some point after melittin tail insertion and before complete breakdown of the liposome. Indeed it may be that increased permeability of the liposomes aids their expansion (via uptake of buffer) prior to their breakdown.

In using the dimensional parameters supplied by DPI to add to the discussion on the models the initial thickness increase (predicted by the carpet model) preceding micellisation leading to large-scale disruption of the vesicular structure leaving behind a 4- to 5-nm-thick lipid bilayer sheet adds further weight to the torridoal model. As the protective effect for DPPC exists at different (higher) concentrations suggests carpet model proceeds via simultaneous carpet forming and degree of insertion.

4.2. Action of melittin on negatively charged liposomes

While a reduction in the lytic activity of melittin on liposomes composed of negatively charged lipids could be expected from results reported in other studies [21,45,46], for example the addition to PC bilayers of molecules, such as dioleoylglycerol, produces large changes in melittin-induced leakage, from 86% for pure PC to 18% for a 8:2 PC/dioleoylglycerol mix [46], measurement of changes in thickness and RI of the immobilised liposomes deliver a new insight into the binding of melittin to liposomes. It has been proposed that the lytic activity of melittin for liposomes was reduced in the presence of negatively charged lipids because of ionic interactions between the positive charges in the peptide and the negative charges on the membrane surface. These interactions have been described as having the effect of anchoring the peptide on the surface and inhibiting its ability to insert into the membrane core region [45]. Fig. 6 reveals the binding of melittin to have at least 2 distinct phases. As with non lysed PC liposomes, phase 1 sees a thickness decrease concurrent with a mass increase, with this 6–8 s period then superseded by a significant thickness increase. The thickness decrease corresponds to a melittin to lipid stoichiometry double that of DPPC at 1:30 (~one melittin per 15 lipid molecules in the outer membrane layer). The postulation that the thickness increase could be due to liposome fusion induced by a cationic peptide was dispelled when the thickness increase was reversed on addition of salt. The reversible thickness and mass increase does provide considerable support for the hypothesis that negatively charged lipids bind melittin via a purely electrostatic mechanism. So initial melittin monomer association can take place with melittin prone within the lipid headgroup region. Increased melittin concentrations within this region do not drive the melittin tail to insert into the lipid bilayer core, but the melittin reorients out of the bilayer to form oligomeric structures with additionally associated melittin standing out from the liposome surface. High salt concentrations are known to induce the formation of melittin tetramers in solution, and it is likely that a similar process can be promoted by the negative charge density at the surface of the lipid bilayer. In this case the large increase in liposome layer thickness is driven by the increased liposome/associated melittin wall thickness for the liposome which is confined within the same surface area, together with melittin coated liposome–liposome repulsion.

Overall, our results provide new details of the mechanism of action of melittin, and specifically for its action in the lysis of vesicles at surfaces. The data we have presented may also be of relevance to the biological action of cytolytic peptides in general.

Acknowledgements

JP wishes to thank the BBSRC for funding under the SBRI initiative. CM would like to thank BBSRC for funding.

References

[1] C.E. Dempsey, The actions of melittin on membranes, Biochim. Biophys. Acta 1031 (1990) 143–161.

[2] E. Habermann, J. Jentsch, Sequence analysis of melittin from tryptic and peptic degradation products, Hoppe-Seyler Z. Physiol. Chem. 348 (1967) 37–50.
[3] L. Yang, T.A. Harroun, T.M. Weiss, L. Ding, H.W. Huang, Barrel-stave model or toroidal model? A case study of melittin pores, Biophys. J. 81 (2001) 1475–1485.
[4] C.R. Dawson, A.F. Drake, J. Helliwell, R.C. Hider, The interaction of bee melittin with lipid bilayer membranes, Biochim. Biophys. Acta 510 (1978) 75–86.
[5] A.S. Ladokhin, S.H. White, Folding of amphipathic alpha-helices on membranes: energetics of helix formation by melittin, J. Mol. Biol. 285 (1999) 1363–1369.
[6] J.H. Kleinschmidt, J.E. Mahaney, D.D. Thomas, D. Marsh, Interactions of Bee Venom melittin with Zwitterionic and negatively charged phospholipid bilayers. A spin-label ESR study, Biophys. J. 72 (1997) 767–778.
[7] S. Kubota, J.T. Yang, Biopolymers 25 (1986) 1493–1504.
[8] Y. Maulet, J.A. Cox, Structural changes in melittin and calmodulin upon complex formation and their modulation by calcium, Biochemistry 22 (1983) 5680–5686.
[9] P. Buckley, A.S. Edison, M.D. Kemple, F.G. Prendergast, The assignments of melittin in methanol, and chemical shift correlations with secondary structure, J. Biomol. NMR 3 (1993) 639–652.
[10] C. Golding, P. O'Shea, The interactions of signal sequences with membranes, Biochem. Soc. Trans. 23 (1995) 971–976.
[11] K.J. Barnham, S.A. Monks, M.G. Hinds, A.A. Azad, R.S. Norton, Solution structure of a polypeptide from the N-terminus of the HIV protein Nef, Biochemistry 36 (1997) 5970–5980.
[12] N.K. Subbarao, R.C. MacDonald, Lipid unsaturation influences melittin-induced leakage of vesicles, Biochim. Biophys. Acta 1189 (1994) 101–107.
[13] H. Raghuraman, Amitabha Chattopadhyay, Influence of lipid chain unsaturation on membrane-bound melittin:a fluorescence approach, Biochim. Biophys. Acta 1665 (2004) 29–39.
[14] K.M. Sekharam, T.D. Badrick, S. Georghiou, Kinetics of melittin binding to phospholipid small unilamellar vesicles, Biochim. Biophys. Acta 1063 (1991) 171–174.
[15] T.D. Badrick, A. Philippetis, S. Georghiou, Stopped-flow fluorometric study of the interaction of melittin with phospholipid bilayers: importance of the physical state of the bilayer and the acyl chain length, Biophys. J. 69 (1995) 1999–2010.
[16] C. Wolfe, J. Cladera, P. O'Shea, Amino acid sequences which promote and prevent the binding and membrane insertion of surface-active peptide: comparison of melittin and promelittin, Mol. Membr. Biol. 15 (1998) 221–227.
[17] N. Papo, Y. Shai, Exploring peptide membrane interaction using surface plasmon resonance: differentiation between pore formation versus membrane disruption by lytic peptides, Biochemistry 42 (2003) 458–466.
[18] H. Vogel, F. Ja¨hnig, The structure of melittin in membranes, Biophys. J. 50 (1986) 573–582.
[19] A.K. Ghosh, R. Rukmini, A. Chattopadhyay, Modulation of Tryptophan environment in membrane-bound melittin by negatively charged phospholipids: implications in membrane organization and function, Biochemistry 36 (1997) 14291–14305.
[20] T.H. Lee, H. Mozsolits, M.I. Aguilar, Measurement of the affinity of melittin for Zwitterionic and anionic membranes using immobilised lipid biosensors, J. Pept. Res. 58 (2001) 464–476.
[21] T. Benachir, M. Lafleur, Study of vesicle leakage induced by melittin, Biochim. Biophys. Acta 1235 (1995) 452–460.
[22] S. Ohki, E. Marcus, D.K. Sukumaran, K. Arnold, Interaction of melittin with lipid membranes, Biochim. Biophys. Acta 1194 (1994) 223–232.
[23] A.S. Ladokhin, S.H. White, Detergent-like permeabilization of anionic lipid vesicles by melittin, Biochim. Biophys. Acta 1514 (2001) 253–260.
[24] G.H. Cross, Y. Ren, N.J. Freeman, Young's fringes from vertically integrated slab waveguides: applications to humidity sensing, Appl. Phys. 86 (1999) 6483–6499.
[25] G.H. Cross, A. Reeves, S. Brand, J.F. Popplewell, L.L. Peel, M.J. Swann, N.J. Freeman, A new quantitative optical biosensor for protein characterisation, Biosens. Bioelectron. 19 (2003) 383–390.
[26] G.H. Cross, A. Reeves, S. Brand, M.J. Swann, L.L. Peel, N.J. Freeman, J.R. Lu, The metrics of surface adsorbed small molecules on the young's fringe dual-slab waveguide interferometer, J. Phys. D: Appl. Phys. 37 (2004) 74–80.
[27] S.J. Biehle, J. Carrozzella, R. Shukla, J.F. Popplewell, M.J. Swann, N.J. Freeman, J.F. Clark, Apolipoprotein E isoprotein specific interactions with tissue plasminogen activator, Biochim. Biophys. Acta, Mol. Basis Dis. 1689 (2004) 244–251.
[28] N.J. Freeman, L.L. Peel, M.J. Swann, J.R. Lu, Lysozyme adsorption studies at the silica–water interface using dual polarisation interferometry, Langmuir 20 (2004) 1827–1832.
[29] L. Saunders, J. Perrin, D. Gammack, Ultrasonic irradiation of some phospholipid sols, J. Pharm. Pharmacol. 14 (1962) 567–572.
[30] A.M. Batenburg, P.E. Bougis, H. Rochat, A.H. Verkleij, B. Dekruijff, Penetration of a cardiotoxin into cardiolipin model membranes and its implications on lipid organization, Biochemistry 24 (1985) 7101–7110.
[31] C. Huang, Studies on phosphatidylcholine vesicles. Formation and physical characteristics, Biochemistry 8 (1) (1969) 344–352.
[32] M. Suenaga, S. Lee, N.G. Park, H. Aoyagi, T. Kato, A. Umeda, K. Amako, Basic amphipathic helical peptides induce destabilization and fusion of acidic and neutral liposomes, Biochim. Biophys. Acta 981 (1989) 143–150.
[33] G. Schwarz, R.T. Zong, T. Popescu, Kinetics of melittin induced pore formation in the membrane of lipid vesicles, Biochim. Biophys. Acta 1110 (1992) 97–104.
[34] H. Mozsolits, H.J. Wirth, J. Werkmeister, M.I. Aguilar, Analysis of antimicrobial peptide interactions with hybrid bilayer membrane systems using surface plasmon resonance, Biochim. Biophys. Acta, Biomembr. 1512 (2001) 64–76.
[35] J.W. Brauner, R. Mendelsohn, F.G. Prendergast, Attenuated total reflectance Fourier transform infrared studies of the interaction of melittin, two fragments of melittin, and-hemolysin with phosphatidylcholines, Biochemistry 26 (1987) 8151–8158.
[36] F. Picard, T. Buffeteau, B. Desbat, M. Auger, M. Pézolet, Quantitative orientation measurements in thin lipid films by attenuated total reflection infrared spectroscopy, Biophys. J. 76 (1999) 539–551.
[37] K.H. Harlos, K. Eible, I. Pascher, S. Sundell, Conformation and packing properties of phosphatidic acid: the crystal structure of monosodium dimyristoylphosphatidate, Chem. Phys. Lipids 34 (1986) 115–126.
[38] M.T. Tosteson, S.J. Holmes, M. Razin, D.C. Tosteson, Melittin lysis of red cells, J. Membr. Biol. 87 (1985) 35–44.
[39] M. Mousli, J.L. Bueb, C. Bronner, B. Rouot, Y. Landry, G protein activation: a receptor-independent mode of action for cationic amphiphilic neuropeptides and venom peptides, Trends Pharmacol. Sci. 11 (1990) 358–362.
[40] K. Matsuzaki, K. Sugishita, N. Ishibe, M. Ueha, S. Nakata, K. Miyajima, R.M. Epand, Relationship of membrane curvature to the formation of pores by magainin 2, Biochemistry 37 (1998) 11856–11863.
[41] H. Lecuyer, D.G. Dervichian, Structure of aqueous mixtures of lecithin and cholesterol, J. Mol. Biol. 45 (1969) 39–57.
[42] D. Allende, S.A. Simon, T.J. McIntosh, Melittin-induced bilayer leakage depends on lipid material properties; evidence for toroidal pores, Biophys. J. 88 (2005) 1–10.
[43] D. Needham, R.S. Nunn, Elastic deformation and failure of lipid membranes containing cholesterol, Biophys. J. 58 (1990) 997–1009.
[44] S. Tristram-Nagle, H.I. Petrache, J.F. Nagle, Structure and interactions of fully hydrated dioleoylphosphatidylcholine bilayers, Biophys. J. 75 (1998) 917–925.
[45] D.K. Hincha, J.H. Crowe, The lytic activity of the bee venom peptide melittin is strongly reduced by the presence of negatively charged phospholipids or chloroplast galactolipids in the membranes of phosphatidylcholine large unilamellar vesicles, Biochim. Biophys. Acta 1284 (1996) 162–170.
[46] M. Monette, M. Lafleur, Modulation of melittin-induced lysis by surface charge density of membranes, Biophys. J. 68 (1995) 187–195.